Japanese Journal of Applied Physics **53**, 060306 (2014) **RAPID COMMUNICATION**
http://dx.doi.org/10.7567/JJAP.53.060306

Enhanced thermoelectric performance of Al-doped ZnO thin films on amorphous substrate

Shrikant Saini[1†], Paolo Mele[1†], Hiroaki Honda[2], Dave J. Henry[3], Patrick E. Hopkins[3], Leopoldo Molina-Luna[4], Kaname Matsumoto[5], Koji Miyazaki[6], and Ataru Ichinose[7]

[1]*Institute for Sustainable Sciences and Development, Hiroshima University, Higashihiroshima, Hiroshima 739-8530, Japan*
[2]*Graduate School for Advanced Sciences of Matter, Hiroshima University, Higashihiroshima, Hiroshima 739-8530, Japan*
[3]*Department of Mechanical and Aerospace Engineering, University of Virginia, Charlottesville, VA 22904, U.S.A.*
[4]*Department of Materials and Geosciences, Technical University of Darmstadt, Darmstadt 64287, Germany*
[5]*Department of Material Science, Kyushu Institute of Technology, Kitakyushu 804-8550, Japan*
[6]*Department of Mechanical Engineering, Kyushu Institute of Technology, Kitakyushu 804-8550, Japan*
[7]*CRIEPI, Electric Power Engineering Research Laboratory, Yokosuka, Kanagawa 240-0196, Japan*
E-mail: ssaini@hiroshima-u.ac.jp; pmele@hiroshima-u.ac.jp

Received March 31, 2014; accepted April 21, 2014; published online May 19, 2014

2% Al-doped ZnO (AZO) thin films fabricated at 300 °C by pulsed laser deposition (PLD) on amorphous fused silica demonstrated the high quality crystallinity and grain connection, which correlates to the high thermoelectric performance: electrical conductivity $\sigma = 923$ S/cm and Seebeck coefficient $S = -111$ μV/K at 600 K. Its power factor ($S^2 \cdot \sigma$) is 1.2×10^{-3} W m^{-1} K^{-2}, twofold better than films deposited on crystalline $SrTiO_3$ under the same experimental conditions. Using our measured thermal conductivity (κ) at 300 K (4.89 W m^{-1} K^{-1}), the figure of merit, $ZT = (S^2 \cdot \sigma \cdot T/\kappa)$, is calculated as 0.045 at 600 K, 5 times larger than ZT of our previously reported bulk ZnO.

Since their discovery in 1822,[1)] thermoelectric materials have attracted significant attention for their ability to directly convert thermal energy to electrical energy without moving parts. The efficiency of thermoelectric energy conversion increases with the dimensionless figure of merit $ZT = S^2 \cdot \sigma \cdot T/\kappa$ (S: Seebeck coefficient; σ: electrical conductivity; κ: thermal conductivity; T: absolute temperature).[2)]

Seminal papers[3,4)] have predicted huge improvements in ZT through quantum confinement in Bi_2Te_3 superlattices. These papers have inspired a wealth of experimental work focused on the production of multiple quantum-well structures, such as multilayered and nanostructured thin films of alloys and intermetallic compounds. Various material systems such as Bi_2Te_3/Sb_2Te_3 multilayers,[5)] layered Zintl phases $Yb_{14}MnSb_{11}$[6)] and AgPbSbTe nanostructured alloys,[7)] have shown remarkable performances, with ZT overcoming 1.5. However, their practical applications remain limited because of low temperature decomposition, presence of rare and often poisonous elements, and high-cost processing. These limitations have stimulated a new focus of research on oxides as alternative thermoelectric materials since they possess important characteristics: environmentally benign nature, abundant supply, cost effectiveness[8)] and thermal stability in air in a wide range of temperatures.

Among sintered oxides, the best thermoelectric performance was obtained with dual Al and Ga doping of ZnO at the Zn site, with $ZT = 0.65$ at 1247 K.[9)] The main obstacle for increasing ZT at the same level of metallic materials has been found in the large values of κ (at room temperature typically 40 W m^{-1} K^{-1} for bulk ZnO vs 0.22 of the Bi_2Te_3/Sb_2Te_3 multilayers). For this reason, several groups have recently started to study the feasibility of nanoengineering control of thermoelectric properties in ZnO thin films[10–13)] and multilayers[14,15)] deposited on crystalline substrates by different techniques like pulsed laser deposition (PLD), molecular beam epitaxy (MBE) and atomic layer deposition (ALD). In particular, we have recently reported[12)] for 2% Al-doped ZnO (AZO) thin films deposited on $SrTiO_3$ single crystals by PLD a large power factor $\sigma \cdot S^2 = 0.55 \times 10^{-3}$ W m^{-1} K^{-2} (600 K), which overcomes the performance of the corresponding our previously reported bulk material[16)] and of all the other films.[10,11,13–15)] In this letter, we extend our previous work, reporting for the first time the enhanced thermoelectric performance of AZO films deposited by PLD on inexpensive amorphous substrates (fused silica). The result is discussed considering the role of deposition temperature on the crystallinity of the films.

The 2% AZO thin films were grown by PLD technique using Nd:YAG laser (266 nm). Pellets of $Zn_{0.98}Al_{0.02}O$ (20 mm in diameter and 3 mm in thickness) prepared by spark plasma sintering were used as the target to grow the thin films. A detailed description of sintered target preparation is reported elsewhere.[16,17)] The laser was shot on the dense AZO target with a energy density of about 4.2 J/cm^2 for a deposition period of 30 min. Thin films were deposited on fused silica substrates at 300, 400, 500, and 600 °C under an oxygen pressure of 200 mTorr. The target was rotated during the irradiation of the laser beam. The substrates were glued with silver paste on an Inconel plate customized for ultrahigh vacuum applications. The thickness of thin films was kept at about 500 nm. Deposition parameters such as pulse frequency (10 Hz), substrate-target distance (about 35 mm) and rotation speed of the target (30% rpm) were kept unchanged during all the deposition routines.

The structural characterization was performed by X-ray diffraction (XRD; Bruker D8 Discover) using Cu Kα radiation ($\lambda = 1.5405$ Å) and morphology was checked by transmission electron microscopy (TEM; JEOL 2010F). The thickness and in-plane roughness were obtained by a Keyence VK-9700 3D microscope. The electrical conductivity was measured from 300–600 K by a custom-built four-point-probe technique consisting of a current source (ADCMT 6144), a temperature controller (Cryo-con 32), and a nano voltmeter (Keithley 2182A). Seebeck coefficient were measured from 300–600 K with a commercially available system (MMR Technologies SB-100). Carrier concentrations and mobilities at room temperature were evaluated by means of Quantum Design PPMS. The thermal conductivities of thin films at room temperature were measured with time domain thermoreflectance (TDTR).[18–20)]

[†]These authors contributed equally to this work.

Table I. Electrical and thermal parameters for thin films and bulk pellet of AZO at 300 K/600 K.

T_{dep} (°C)	Grain size (nm)	Electrical conductivity σ (S/cm)	Carrier concentration n (10^{19} cm^{-3})	Mobility μ (cm^2 V^{-1} s^{-1})	Seebeck coefficient S (μV/K)	Power factor PF (10^{-3} W m^{-1} K^{-2})
300	60	601/923	0.23	950	−62/−114	0.23/1.2
400	90	74/93	0.22	206	−119/−203	0.11/0.37
500	90	38/54	1.70	13	−141/−236	0.08/0.30
600	120	20/27	0.01	1730	−139/−220	0.04/0.13
Bulk AZO[a)]	—	206/152	—	—	−132/−150	0.35/0.34

a) Refs. 17 and 25.

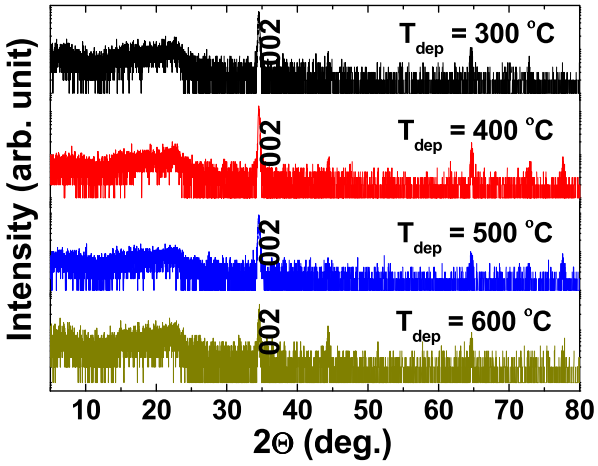

Fig. 1. (Color online) XRD patterns of AZO films deposited at different temperatures (T_{dep} = 300, 400, 500, and 600 °C).

All the films deposited on fused silica have wurtzite hexagonal structure and are *c*-axis oriented since only (002) peak appears in XRD θ–2θ scan (Fig. 1). The *c*-axis length is about 5.19 Å, independent of deposition temperature, and slightly compressed with respect to bulk (5.20 Å). Off-axis scans (φ-scan) along the (002) axis of the thin films do not show any peaks which indicates that nanocrystalline grains are randomly distributed in plane, maintaining their *c*-axis perpendicular to the substrate surface. According to SEM analysis of the film surfaces (not reported here), the grain size increases with deposition temperature, as reported in Table I.

Transport and thermoelectric properties of AZO thin films are summarized in Table I and Fig. 2. Figure 2(a) shows the electrical conductivity vs temperature for AZO thin films deposited at various substrate temperatures (300, 400, 500, and 600 °C). All the films show typical semiconducting behavior. The increasing deposition temperature leads to a decrease of electrical conductivity. At 600 K, the film deposited at 300 °C shows the highest electrical conductivity (923 S/cm, threefold greater than values reported on single crystals[12)]) while the film deposited at 600 °C shows the lowest electrical conductivity, 27 S/cm at room temperature, even lower than our previously reported bulk material (152 S/cm).[16)] The values of carrier concentrations and mobilities, determined by Hall measurements, are reported in Table I. Similarly as in the samples deposited on crystalline substrates,[17)] it is not possible to find a clear correlation between the carrier concentration, the mobility and the electrical conductivity. Figure 2(b) shows the Seebeck coefficient of the thin films over the temperature range from 300 to 600 K. The films show a negative Seebeck coefficient, which indicates n-type conduction due to Al^{3+} doping and oxygen vacancies. The absolute value of the Seebeck coefficient increases with deposition temperature and operating temperature as well. The highest value of the Seebeck coefficient at 600 K is −236 μV/K for thin films deposited at 600 °C and the lowest −114 μV/K for thin films deposited at 300 °C, which is opposite behavior with respect to electrical con-

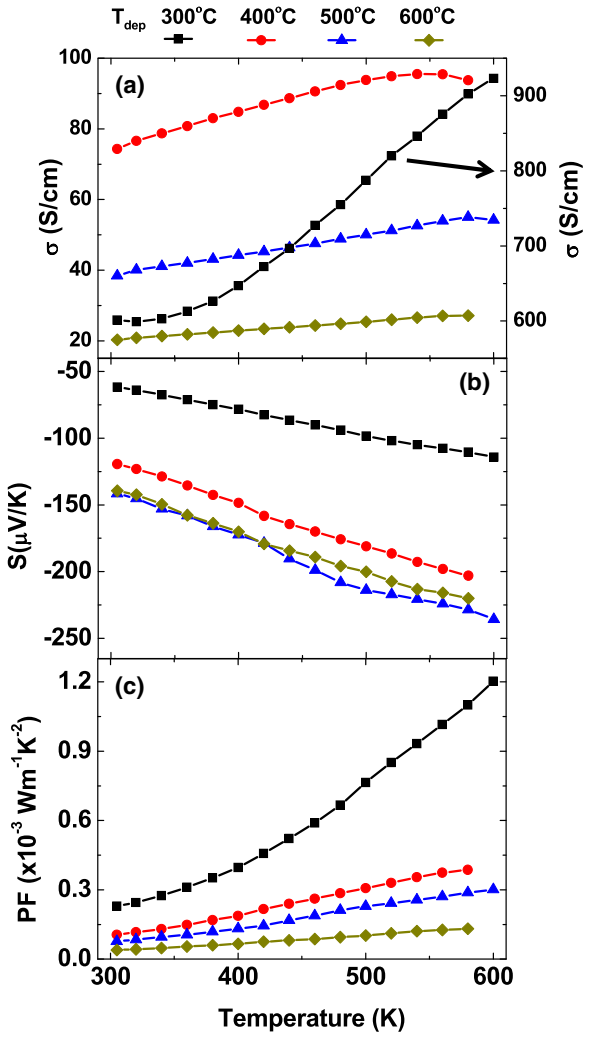

Fig. 2. (Color online) (a) Electrical conductivity vs temperature (σ–T) characteristics, (b) Seebeck coefficient vs temperature (S–T) characteristics, (c) power factor vs temperature (PF–T) characteristics of AZO thin films deposited at different temperature (T_{dep} = 300, 400, 500, and 600 °C).

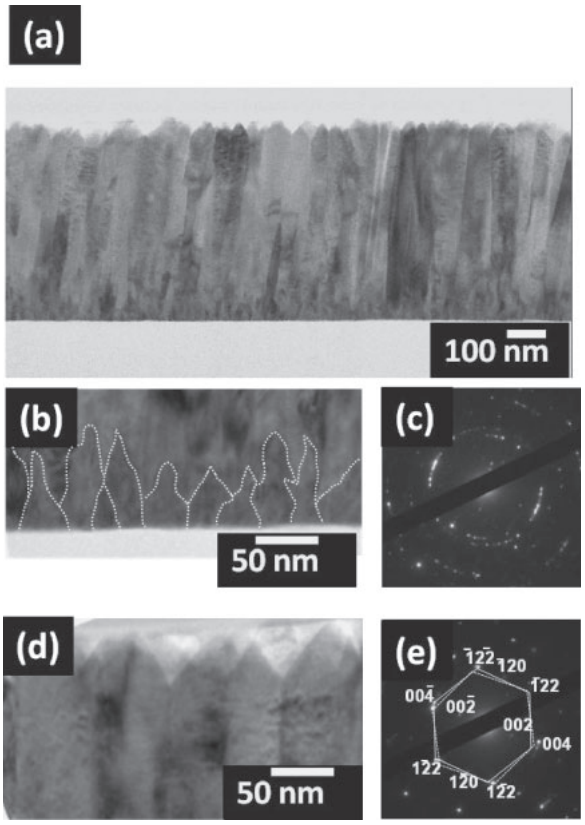

Fig. 3. TEM and electron diffraction patterns of AZO films deposited at $T_{dep} = 300\,°C$. (a) High-magnification cross sectional TEM image; (b) higher magnification of the bottom layer: grain boundaries are evidenced by dotted line; (c) electron diffraction pattern taken along the [100] direction in the bottom layer; (d) higher magnification of the top layer showing columnar grains; (e) electron diffraction pattern taken along the [100] in the top layer: crystallographic indexes are reported for one of the two tilted subsystems.

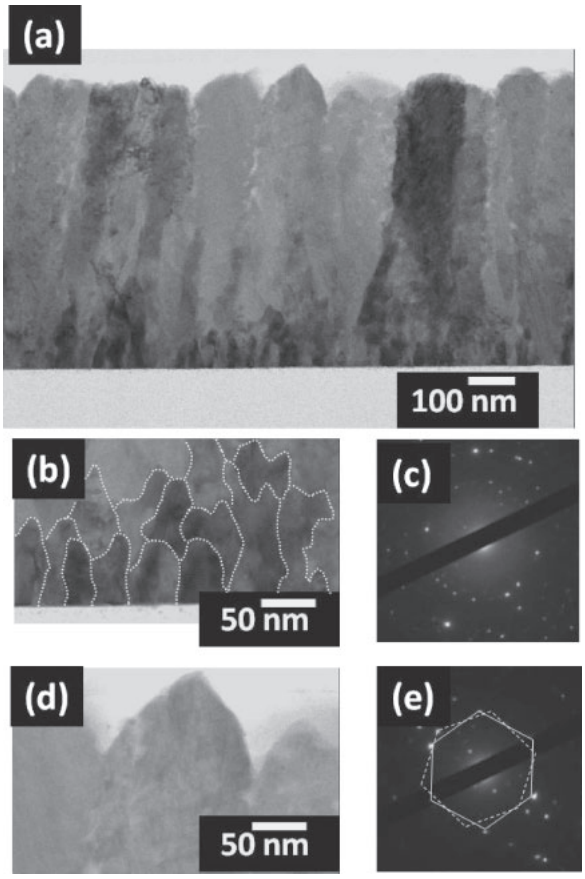

Fig. 4. TEM and electron diffraction patterns of AZO films deposited at $T_{dep} = 600\,°C$. (a) High-magnification cross sectional TEM image; (b) higher magnification of the bottom layer: grain boundaries are evidenced by dotted line; (c) electron diffraction taken along the [100] direction in the bottom layer; (d) higher magnification of the top layer showing columnar grains; (e) electron diffraction taken along [100] in the top layer with evidence of two tilted hexagonal subsystems.

ductivity. The Seebeck coefficients of AZO/silica films present similar values and dependence with deposition temperature as AZO/$SrTiO_3$ films.[12)]

From the values of Seebeck coefficient and electrical conductivity, we have calculated the efficiency of thermoelectric material by the value of power factor (PF) of thin films as $PF = S^2 \cdot \sigma$ [Fig. 2(c)]. The value of power factor decreases with deposition temperature and increases with operating temperature. Thin films deposited at 300 °C demonstrate the highest value of power factor: $0.23 \times 10^{-3}\,W\,m^{-1}\,K^{-2}$ at 300 K and $1.2 \times 10^{-3}\,W\,m^{-1}\,K^{-2}$ at 600 K. Due to the high electrical conductivity value, the thermoelectric performance of thin films deposited at 300 °C is enhanced in comparison with previous reports for thin films ($0.55 \times 10^{-3}\,W\,m^{-1}\,K^{-2}$ at 600 K on $SrTiO_3$[12)]).

The remarkable difference between the performances of best (deposited at 300 °C) and worst (deposited at 600 °C) AZO/silica samples can be explained comparing the morphology and orientations of the grains. Cross-sectional TEM observation [Figs. 3(a) and 4(a)] clearly show the same morphology for both films: columnar grains grow on a thin seed layer constituted by smaller grains, similarly as observed earlier by other groups[13,21)] for AZO films grown on glass. According to energy-dispersive X-ray spectroscopy (EDS) analysis, the smaller grains are constituted by Al, Zn, and O. We can exclude any interfacial reactions between AZO and silica. Interestingly, on single crystalline substrates the seed layer was never observed and the columnar grains grow directly on the substrate. Closer inspection [Figs. 3(b) and 4(b)] reveals that the grains width are 20–50 nm for both films, though the thickness of the seed layer, about 60 nm for the sample deposited at 300 °C, doubles at 600 °C. Electron diffraction shows ring shaped patterns [Figs. 3(c) and 4(c)], which the signature of randomly oriented grains. The length of the columnar grain layer is about 500 nm for the film deposited at 300 °C and 600 nm for the other films. Widths are about 60 nm for the film deposited at 300 °C and 120 nm for the other film, consistent with the observation from the SEM (Table I). The columnar grains of the first sample are well connected and grain boundaries are sharp [Figs. 3(a) and 3(d)], while the second sample presents several pores at the grain boundaries [Figs. 4(a) and 4(d)]. Consequently, electron scattering is expected to be larger in the second samples, and this qualitatively explains the differences in electrical conductivity. Furthermore, both films show two hexagonal electron diffraction patterns [Figs. 3(e) and 4(e)] tilted from the ideal orientation (perpendicular to the surface of the substrate), however tilt is much more evident in the film deposited at 600 °C. This is another proof of the superior crystallinity of the sample deposited at 300 °C. TEM and electron diffraction patterns are not available for the samples deposited at 400 and

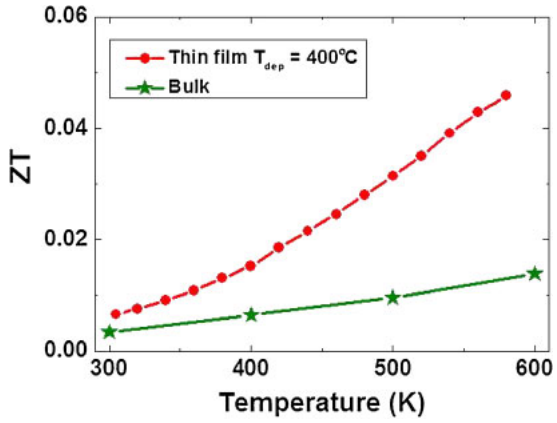

Fig. 5. (Color online) Dimensionless figure of merit at elevated temperatures using thermal conductivity at 300 K for AZO thin film deposited at 400 °C compared with our previously reported bulk material[16] of same composition.

500 °C. However, considering the trend of grain size (Table I) and XRD patterns (Fig. 1) it seems reasonable to explain their intermediate thermoelectric performances with intermediate crystallinity and grain connection.

The improved performance of the AZO/silica film in comparison with films deposited on single crystals under the same experimental conditions may be explained by invoking lower density of dislocations, according with the study done by Novotny et al.[22] The reasons for the limited amount of dislocations are the lowest stress of thin films deposited on fused silica (0.9 GPa) and lower electron density in interatomic regions.[22] Being that silica is amorphous, it is not possible to calculate the linear density of dislocations for a comparison with the films grown on single crystals. Direct observation of strain at the nanoscale by advanced methods like Geometrical Phase Analysis[23] are planned to validate the dislocation argument.

The thermal conductivity (κ) for AZO thin film deposited at 400 °C is $4.89 \pm 0.81\,\mathrm{W\,m^{-1}\,K^{-1}}$ at 300 K, one order of magnitude lower than for our previously reported bulk AZO at room temperature,[16] and consistent with values reported by other groups.[13,20] The dimensionless figure of merit ZT is calculated as about 0.0067. The behavior of ZT values for thin films at elevated temperatures is estimated using κ at 300 K (κ_{300K}) as the thermal conductivity; since the thermal conductivity of crystals decreases with increasing temperature due to increased phonon–phonon scattering, we assert this as a conservative approximation.[24] Figure 5 shows that ZT of the AZO films is always higher than for our previously reported bulk of the same composition[16] for all temperatures in the range considered in this study. For instance, ZT at 600 K is 0.045, with an enhancement of about five times with respect to our previously reported bulk.[16] This result is quite encouraging for the practical applications of thermoelectric oxide thin films.

In summary, the thermoelectric material AZO was grown as thin film by pulsed laser deposition technique at various deposition temperatures ($T_{dep} = 300$, 400, 500, and 600 °C) on cheap amorphous fused silica substrates. All thin films are crystalline with preferential c-axis orientation. Over the temperature range from 300–600 K, the thin film deposited at 300 °C clearly shows the best thermoelectric performance: $\sigma = 932\,\mathrm{S/cm}$, $S = -144\,\mu\mathrm{V/K}$, and PF $(= S^2 \cdot \sigma) = 1.2 \times 10^{-3}\,\mathrm{W\,m^{-1}\,K^{-2}}$ at 600 K, better than AZO films deposited on single crystals. This result is due to two facts: excellent grain connectivity and superior crystallinity of the sample deposited at 300 °C. Thermal conductivity is $4.89 \pm 0.81\,\mathrm{W\,m^{-1}\,K^{-1}}$ at room temperature. From this, we conservatively estimate the thermoelectric figure of merit of our AZO thin films as $ZT = 0.045$ at 600 K, fivefold better than our previously reported bulk material of same composition. Since silica is much cheaper than single crystalline substrates, this result is quite encouraging for the practical applications of thermoelectric oxide thin films.

Acknowledgments We thank Dr. J. F. Ihlefeld of Sandia National Laboratories for insightful discussions. D.J.H. and P.E.H. are appreciate funding from the United States National Science Foundation, Grant. No. CBET-1339436 and the Commonwealth Research Commercialization Fund (CRCF) of Virginia.

1) T. J. Seebeck, Abh. Akad. Wiss. Berlin, 289 (1822).
2) H. Böttner, MRS Proc. **1166**, N01-01 (2009).
3) L. D. Hicks and M. S. Dresselhaus, Phys. Rev. B **47**, 12727 (1993).
4) L. D. Hicks and M. S. Dresselhaus, Phys. Rev. B **47**, 16631 (1993).
5) R. Venkatasubramanian, E. Siivola, T. Colpitts, and B. O'Quinn, Nature **413**, 597 (2001).
6) E. S. Toberer, A. F. May, and G. J. Snyder, Chem. Mater. **22**, 624 (2010).
7) M. Kanatzidis, Chem. Mater. **22**, 648 (2010).
8) K. Koumoto, I. Terasaki, and R. Funahashi, MRS Bull. **31** [3], 206 (2006).
9) M. Ohtaki, K. Araki, and K. Yamamoto, J. Electron. Mater. **38**, 1234 (2009).
10) N. Vogel-Schäuble, Y. E. Romanyuk, S. Yoon, K. J. Saji, S. Populoh, S. Pokrant, M. H. Aguirre, and A. Weidenkaff, Thin Solid Films **520**, 6869 (2012).
11) A. I. Abutaha, S. R. Sarath Kumar, and H. N. Alshareef, Appl. Phys. Lett. **102**, 053507 (2013).
12) P. Mele, S. Saini, H. Honda, K. Matsumoto, K. Miyazaki, H. Hagino, and A. Ichinose, Appl. Phys. Lett. **102**, 253903 (2013).
13) N. Vogel-Schäuble, T. Jaeger, Y. E. Romanyuk, S. Populoh, C. Mix, G. Jakob, and A. Weidenkaff, Phys. Status Solidi: Rapid Res. Lett. **7**, 364 (2013).
14) T. Tynell, I. Terasaki, H. Yamauchi, and M. Karppinen, J. Mater. Chem. A **1**, 13619 (2013).
15) M. Ruoho, V. Pale, M. Erdmanis, and I. Tittonen, Appl. Phys. Lett. **103**, 203903 (2013).
16) P. Mele, H. Kamei, H. Yasumune, K. Matsumoto, and K. Miyazaki, Met. Mater. Int. **20**, 389 (2014).
17) P. Mele, K. Matsumoto, T. Azuma, K. Kamesawa, S. Tanaka, J. Kurosaki, and K. Miyazaki, MRS Proc. **1166**, 3 (2009).
18) D. G. Cahill, K. Goodson, and A. Majumdar, J. Heat Transfer **124**, 223 (2002).
19) A. J. Schmidt, X. Chen, and G. Chen, Rev. Sci. Instrum. **79**, 114902 (2008).
20) P. E. Hopkins, J. R. Serrano, L. M. Phinney, S. P. Kearney, T. W. Grasser, and C. T. Harris, J. Heat Transfer **132**, 081302 (2010).
21) S.-Y. Lee, W. Lee, C. Nahm, J. Kim, S. Byun, T. Hwang, B.-K. Lee, Y. I. Jang, S. Lee, H.-M. Lee, and B. Park, Curr. Appl. Phys. **13**, 775 (2013).
22) M. Novotny, J. Cizek, R. Kuzel, J. Bulir, J. Lancok, J. Connolly, E. McCarthy, S. Krishnamurthy, J.-P. Mosnier, W. Anwand, and G. Brauer, J. Phys. D **45**, 225101 (2012).
23) M. J. Hÿtch, E. Snoeck, and R. Kilaas, Ultramicroscopy **74**, 131 (1998).
24) G. S. Nolas and H. J. Goldsmid, *Thermal Conductivity: Theory, Properties and Applications* (Kluwer Academic/Plenum, New York, 2004) p. 114.
25) For bulk AZO, the value of S, σ, and power factor at 300 K are taken by extrapolation of S and σ from Ref. 17.